



Different Conformations of 1-Deazaadenosine and its 2'-Deoxyribonucleoside in the Solid State and in Solution

Frank Seela^{a*}, Harald Debelak^a, Hans Reuter^b, Guido Kastner^b, and Igor A. Mikhailopulo^a

^a *Laboratorium für Organische und Bioorganische Chemie, Institut für Chemie, Universität Osnabrück, Barbarastr. 7, D-49069 Osnabrück, Germany*

^b *Anorganische Chemie, Institut für Chemie, Universität Osnabrück, Barbarastr. 7, D-49069 Osnabrück, Germany*

Received 19 October 1998; accepted 3 December 1998

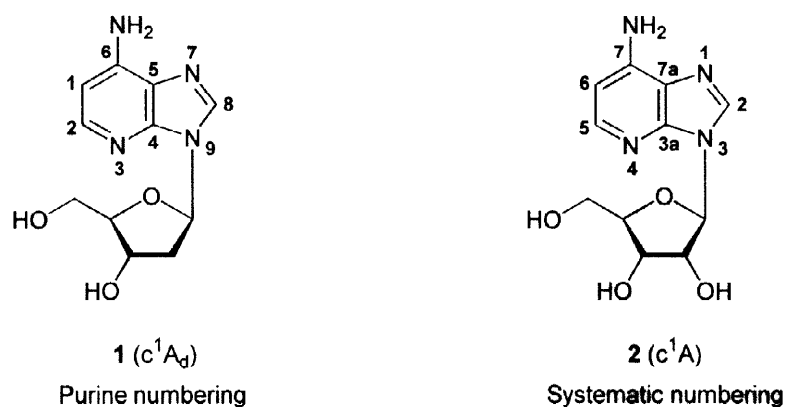
ABSTRACT — Crystallization of 1-deaza-2'-deoxyadenosine (c^1A_d , **1**) from propanol-2 gives two forms of crystals: type **A** formed firstly as plates, then, on the surface of the plates, type **B** appeared as needles. Single crystal X-ray analyses shows that the crystals **A** and **B** differ mainly in the sugar ring conformation: **A** adopts the S-type ($P = 179.8^\circ$; C-2'-*endo*-C-3'-*exo*; 2T_3) conformation associated with an *high-anti* base orientation ($\chi = -90.7^\circ$) and the $\gamma = 152.3^\circ$ across the exocyclic C(4')-C(5') bond; **B** shows N-type ($P = 21.2$; C-3'-*endo*; 3E) conformation accompanied by a somewhat different *anti* base orientation ($\chi = -116.5^\circ$) an eclipsed orientation of the exocyclic C(4')-C(5') bond ($\gamma = 84.5^\circ$). No intramolecular hydrogen bonds in both types of crystals can be detected. Unlike c^1A_d , the ribonucleoside (c^1A , **2**) is in the *syn* conformation ($\chi = 56.1^\circ$) in the solid state which is caused by an intramolecular (5')CH₂OH...N(3) hydrogen bond. The compounds **1** and **2** display very similar conformation in D₂O solution with a strong preference for the S-type conformation of the furanose ring accompanied by the intramolecular (5')CH₂OH...N(3) hydrogen bond. © 1999 Published by Elsevier Science Ltd. All rights reserved.

Keywords: X-Ray crystal structures, nucleosides, conformation, 1-deazaadenosine, 1-deaza-2'-deoxyadenosine.

INTRODUCTION

The nucleosides of 1-deazaadenine (imidazo[4,5-b]pyridine) are strong inhibitors of adenosine deaminase [1,2] and display a broad spectrum of affinity for adenosine receptors [3,4]. Oligonucleotides containing 1-deaza-2'-deoxyadenosine (c^1A_d , **1**) or 1-deaza-adenosine (c^1A , **2**) show unusual structures with a preference for Hoogsteen base pairing [5-8] and were used as a structural probes for the hammerhead ribozyme [9].

The structural and conformational properties of 1-deazaadenine nucleosides are expected to be closely related to their biochemical properties. It was previously demonstrated for 3'-*O*-methyl-1-deazaadenosine that forms the *syn*-conformer in the solid state is stabilized by a hydrogen bond between the 5'-hydroxyl group and the nitrogen-3 [10]. It was also shown that the N-glycosylic bond conformation of 1-deazapurine nucleosides strongly depends on the nature of the 6-substituents and a linear correlation of the *syn*-conformer population vs. the σ_{para} Hammett constants for the 6-substituents were established [11]. This can be considered to be the result of the increased π -electron density of the pyridine system compared to the pyrimidine moiety of purine nucleosides. In this study the crystal structure of 1-deaza-2'-deoxyadenosine (c^1A_d , **1**) is determined and compared to that of 1-deazaadenosine. A conformational analysis is also performed in solution by ^1H NMR spectroscopy.



RESULTS AND DISCUSSION

Conformation in the solid state

The structures of c^1A_d , (**1**) and c^1A , (**2**) as observed in the case of single crystal X-ray diffraction are shown in the Figures 1 and 2, respectively. Surprisingly, slow crystallization of the 2'-deoxyribonucleoside gave two forms of crystals whereas the ribonucleoside formed only one type. The c^1A_d crystallizes from propanol-2 first in compact plates and then in thin, needle-shaped crystals. The crystal parameters are summarized in the Experimental. Bond lengths and angles for the two forms of crystals of c^1A_d (**A**,**B**) and for c^1A are listed in the Tables 1 and 2, selected torsion angles in Table 3. Both crystal structures do not contain any solvent molecules.

In the compact crystals of c^1A_d (**A**) both hydrogen atoms of the N(6) amino group form intermolecular hydrogen bonds to the hydroxyl group oxygens of two neighbouring molecules: one of them binds to O(3') [$d(\text{H}\cdots\text{O}) = 2.199 \text{ \AA}$, angle (N-H \cdots O) = 171.04°], the other binds to O(5') in a second symmetry equivalent molecule [$d(\text{H}\cdots\text{O}) = 2.268 \text{ \AA}$, angle (N-H \cdots O) = 140.46°]. The hydrogen atoms of these hydroxyl groups are

also involved in hydrogen bonds, viz., H(3'O) bonds to O(4') in a third neighbouring molecule [$d(\text{H}\cdots\text{O}) = 2.125 \text{ \AA}$, angle $(\text{O}-\text{H}\cdots\text{O}) = 142.95^\circ$], H(5'O) bonds to the N(3) nitrogen atom of the base in the same neighboring molecule [$d(\text{H}\cdots\text{N}) = 1.955 \text{ \AA}$, angle $(\text{O}-\text{H}\cdots\text{N}) = 168.63^\circ$].

In the needle-shaped crystals of c^1A_d (B) only one of the two hydrogen atoms of the N(6) amino function is involved in hydrogen bonding with the O(3') atom in a neighbouring molecule [$d(\text{H}\cdots\text{O}) = 2.101 \text{ \AA}$, angle $(\text{N}-\text{H}\cdots\text{O}) = 160.58^\circ$]. The hydroxyl groups do not form hydrogen bonds to other hydroxyl groups but to nitrogen atoms of the bases in two more neighbouring molecules. The hydrogen atom H(3'O) of the O(3') hydroxyl group bonds to N(7) [$d(\text{H}\cdots\text{N}) = 1.910 \text{ \AA}$, angle $(\text{O}-\text{H}\cdots\text{N}) = 176.35^\circ$]. The H(5'O) of the O(5') hydroxyl group is linked to N(3) [$d(\text{H}\cdots\text{N}) = 2.023 \text{ \AA}$, angle $(\text{O}-\text{H}\cdots\text{N}) = 161.06^\circ$].

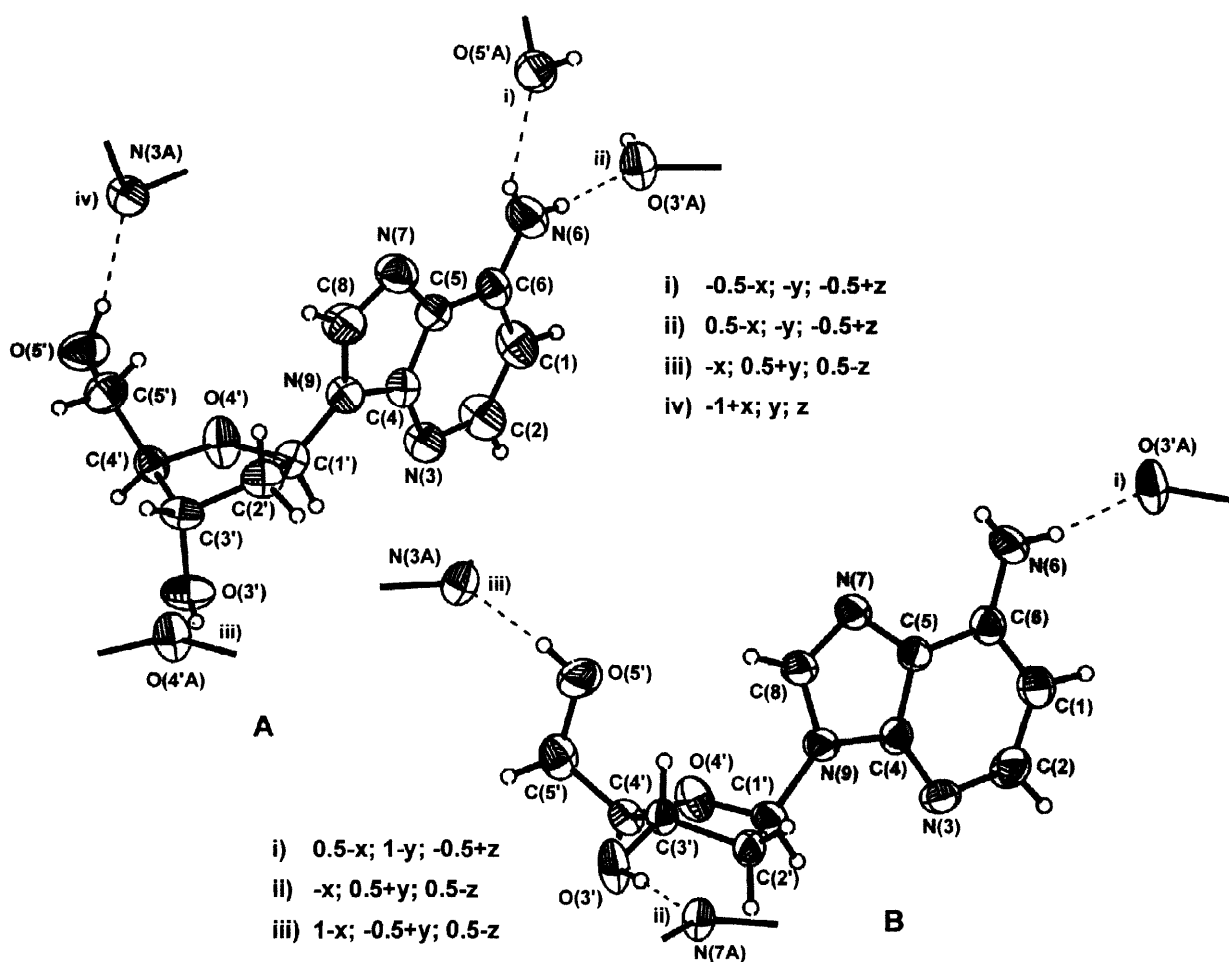


Figure 1. Perspective view (thermal ellipsoids at 50% probability level) of two forms A and B of c^1A_d (1).

The ribonucleoside *c'*A (2) crystallizes from water as a monohydrate. The crystal structure is stabilized by hydrogen bonds. The solvent molecule acts as a donor and a receptor of two hydrogen bonds. In the donor case, the hydrogen atoms of H₂O are bonded to the N(6) nitrogen atom and to a O(3') hydroxyl hydrogen atom in two neighbouring molecules. The H...O distances are 2.336 Å for H(61) and 2.068 Å for H(3'O), respectively; the N-H...O angle is 154.42°, the O-H...O angle is 144.25°. The hydrogen atoms of the water molecule are coordinated to an oxygen atom O(4') in the sugar unit and to N(7), a nitrogen atom of the base of two more nucleoside molecules. The H...O distance is 1.981 Å [H(102)], the H...N distance is 2.068 Å [H(101)]. The O-H...O and O-H...N angles of these hydrogen bonds are 161.31° and 165.87°, respectively.

The remaining hydrogen atom of the amino function forms a hydrogen bond to the O(2') oxygen atom of a hydroxyl group in a neighbouring molecule [$d(\text{H}\cdots\text{O}) = 2.196 \text{ \AA}$, angle (N-H...O) = 149.74°]. This O(2') hydroxyl group itself is bonded *via* H(2'O) to an O(5') hydroxyl oxygen atom in a neighboring molecule [$d(\text{H}\cdots\text{O}) = 2.030 \text{ \AA}$, angle (O-H...O) = 152.44°].

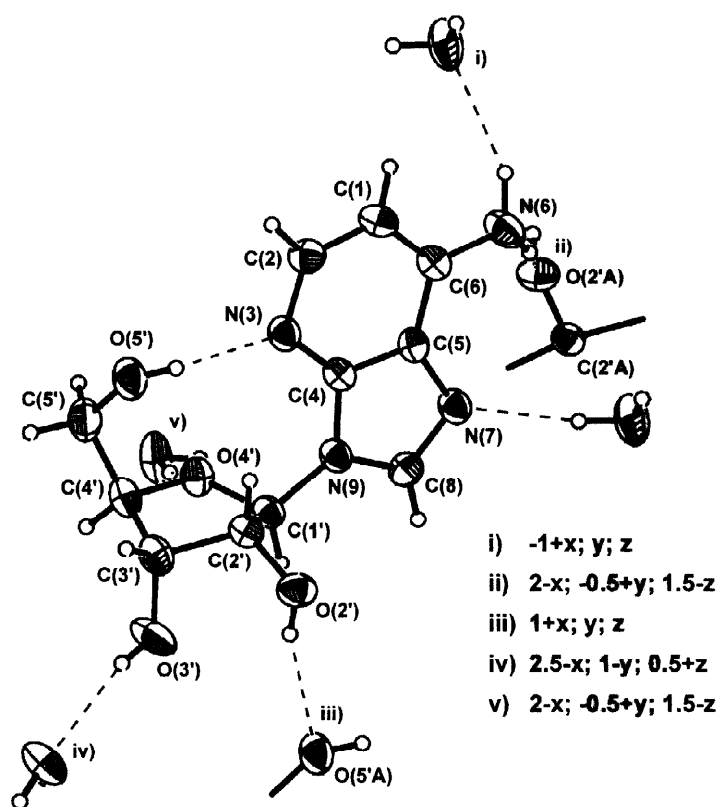


Figure 2. Perspective view (thermal ellipsoids at 50% probability level) of 1-deazaadenosine (2).

Table 1. Bond lengths (Å) of the 1-deaza-2'-deoxyadenosine (**1**, two forms of crystals: plates and needles) and 1-deazaadenosine (**2**)^a.

Bond	c ¹ A _d (A, plates)	c ¹ A _d (B, needles)	c ¹ A·H ₂ O (2)
C(1)-C(2)	1.375(6)	1.388(5)	1.388(4)
C(1)-C(6)	1.400(5)	1.407(5)	1.392(4)
C(2)-N(3)	1.346(5)	1.343(4)	1.344(4)
N(3)-C(4)	1.336(4)	1.338(4)	1.330(3)
C(4)-N(9)	1.382(4)	1.389(4)	1.390(3)
C(4)-C(5)	1.387(5)	1.387(4)	1.396(3)
C(5)-N(7)	1.395(4)	1.390(4)	1.388(3)
C(5)-C(6)	1.398(5)	1.406(4)	1.405(4)
C(6)-N(6)	1.349(4)	1.357(4)	1.368(3)
N(7)-C(8)	1.304(5)	1.307(4)	1.309(3)
C(8)-N(9)	1.374(4)	1.371(4)	1.364(3)
N(9)-C(1')	1.441(4)	1.465(4)	1.453(3)
C(1')-O(4')	1.427(4)	1.412(4)	1.414(3)
C(1')-C(2')	1.519(4)	1.534(4)	1.534(3)
C(2')-O(2')	–	–	1.406(3)
C(2')-C(3')	1.511(5)	1.524(4)	1.530(4)
C(3')-O(3')	1.431(4)	1.418(4)	1.421(4)
C(3')-C(4')	1.523(4)	1.526(4)	1.526(4)
C(4')-O(4')	1.437(4)	1.447(4)	1.460(3)
C(4')-C(5')	1.503(5)	1.497(5)	1.511(4)
C(5')-O(5')	1.421(4)	1.422(4)	1.418(4)

^a Purine numbering.

A comparison of the two crystal structures (A and B) show that the 2'-deoxyribonucleoside **1** exhibits different N-glycosylic bond conformations (A, $\chi = -90.7^\circ$; B, $\chi = -116.5^\circ$). They display no intramolecular hydrogen bonds and differ mainly in the sugar ring conformation (Table 3). In the compact crystals the sugar moiety shows the S-type sugar puckering ($P = 179.8^\circ$; C-2'-endo-C-3'-exo; 2T_3) with a puckering amplitude $\phi_m = 36.4^\circ$, whereas the N-type sugar puckering ($P = 21.2^\circ$; C-3'-endo; 3E ; $\phi_m = 33.6^\circ$) characterizes the needle-shaped crystals. Both crystal structures, A and B, display different conformations about the C(4')-C(5') bond, viz., the former is in the *ap* [(-)*gauche*; -*g*] conformation ($\gamma = 177.9^\circ$), whereas the latter is in the +*sc* [(+)*gauche*; +*g*] conformation ($\gamma = 46.8^\circ$).

Different from both crystal structures of c¹A_d, one intramolecular hydrogen bond was found in the crystal structure of the ribonucleoside c¹A, namely between H(5'O) hydrogen atom and the N(3) nitrogen atom of the base [$d(\text{H}\cdots\text{N}) = 1.928 \text{ \AA}$, angle (O-H \cdots N) = 173.9°] which causes *syn* conformation (Fig. 2).

The pentofuranose moiety of c^1A adopts the S-type conformation ($P = 167.5^\circ$; C-2'-*endo*; 2E ; $\phi_m = 37.6^\circ$) with the +*sc* [(+)*gauche*; +*g*] orientation of the exocyclic C(4')-C(5') bond ($\gamma = 46.6^\circ$). Moreover, c^1A and structure **B** of c^1A_d display a close similarity in the orientation about the C(4')-C(5') bond albeit the latter structure is not stabilized by an intramolecular hydrogen bond.

The heterocyclic bases of both compounds are fairly planar showing maximal deviations of their carbon and nitrogen atoms from the least-squares plane in the range of +0.017 / -0.032 Å (c^1A), +0.012 / -0.007 Å (c^1A_d , plates), and +0.006 / -0.006 Å (c^1A_d , needles).

Table 2. Bond angles ($^\circ$) of 1-deaza-2'-deoxyadenosine (**1**) and 1-deazaadenosine (**2**)^a.

Bond angle	c^1A_d (A, plates)	c^1A_d (B, needles)	$c^1A \cdot H_2O$ (2)
C(2)-C(1)-C(6)	120.8(3)	120.6(3)	121.7(2)
N(3)-C(2)-C(1)	126.3(3)	126.2(3)	124.7(2)
C(4)-N(3)-C(2)	111.6(3)	111.8(3)	112.8(2)
N(3)-C(4)-N(9)	126.5(3)	126.9(3)	127.4(2)
N(3)-C(4)-C(5)	127.5(3)	127.9(3)	127.6(2)
N(9)-C(4)-C(5)	106.0(3)	105.2(2)	105.1(2)
N(7)-C(5)-C(4)	110.4(3)	110.4(2)	110.6(2)
N(7)-C(5)-C(6)	130.2(3)	130.4(3)	130.8(2)
C(4)-C(5)-C(6)	119.4(3)	119.2(3)	118.6(2)
N(6)-C(6)-C(1)	123.2(3)	123.4(3)	123.1(3)
N(6)-C(6)-C(5)	122.4(3)	122.3(3)	122.3(2)
C(1)-C(6)-C(5)	114.4(3)	114.3(3)	114.5(2)
C(8)-N(7)-C(5)	103.7(3)	104.8(2)	104.1(2)
N(7)-C(8)-N(9)	114.6(3)	113.2(3)	114.3(2)
C(8)-N(9)-C(4)	105.2(3)	106.3(2)	106.0(2)
C(8)-N(9)-C(1')	128.9(3)	126.7(2)	126.6(2)
C(4)-N(9)-C(1')	125.4(2)	126.3(2)	127.3(2)
O(4')-C(1')-N(9)	108.6(2)	107.7(3)	108.2(2)
O(4')-C(1')-C(2')	105.9(2)	107.5(2)	105.4(2)
N(9)-C(1')-C(2')	116.7(3)	114.4(3)	115.4(2)
O(2')-C(2')-C(3')	–	–	115.2(2)
O(2')-C(2')-C(1')	–	–	113.4(2)
C(3')-C(2')-C(1')	102.2(2)	103.0(2)	101.2(2)
O(3')-C(3')-C(4')	107.0(2)	109.1(2)	109.5(2)
O(3')-C(3')-C(2')	111.3(3)	114.2(2)	107.8(2)
C(4')-C(3')-C(2')	102.6(2)	102.8(2)	102.8(2)
O(4')-C(4')-C(5')	109.8(3)	109.6(3)	109.0(2)
O(4')-C(4')-C(3')	105.2(2)	104.6(2)	105.4(2)
C(5')-C(4')-C(3')	114.5(3)	116.1(3)	116.1(2)
C(1')-O(4')-C(4')	110.6(2)	110.5(2)	110.5(2)
O(5')-C(5')-C(4')	109.0(3)	110.5(3)	113.8(2)

^a Purine numbering.

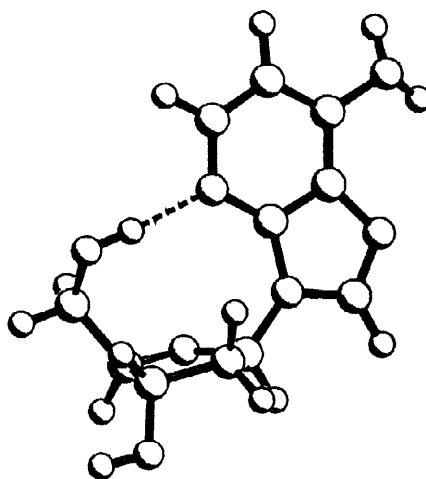
Table 3. Torsion angles ($^{\circ}$) and the Altona-Sundaralingam parameters of the sugar moieties of 1-deaza-2'-deoxyadenosine (**1**, two forms: plates and needles) and 1-deazaadenosine (**2**).

Torsion angle ^a		c ¹ A _d (A)	c ¹ A _d (B)	c ¹ A (2)
C(4')-O(4')-C(1')-C(2')	ν_0	-11.9(3)	-1.6(3)	-19.9(3)
O(4')-C(1')-C(2')-C(3')	ν_1	30.3(3)	-19.2(3)	35.3(2)
C(1')-C(2')-C(3')-C(4')	ν_2	-36.4(3)	31.3(3)	-36.7(3)
C(2')-C(3')-C(4')-O(4')	ν_3	30.2(3)	-33.0(3)	26.1(3)
C(3')-C(4')-O(4')-C(1')	ν_4	-11.6(3)	21.9(3)	-4.0(3)
O(5')-C(5')-C(4')-C(3')	γ	177.9(3)	46.8(4)	46.6(4)
O(5')-C(5')-C(4')-O(4')		59.9(4)	-71.4(3)	-72.2(3)
C(5')-C(4')-C(3')-O(3')	δ	152.3(3)	84.5(3)	151.0(2)
O(4')-C(1')-N(9)-C(4)	χ	-90.7(4)	-116.5(3)	56.1(3)
O(4')-C(1')-N(9)-C(8)		79.4(4)	52.7(4)	-119.0(3)
Phase angle	P	179.8 (³ T ₂ ; S)	21.2 (³ E; N)	167.5 (² E; S)
Puckering amplitude	ϕ_m	36.4	33.6	37.6

^a Purine numbering.

Conformation in solution

Both compounds, c¹A (**1**) and c¹A_d (**2**), display very similar conformation in D₂O and DMSO solutions with a strong preference for the S-type conformation of the furanose ring accompanied by the intramolecular (5')CH₂OH...N(3) hydrogen bond (Fig. 3).

Figure 3. The most populated conformation of c¹A_d (**1**) in aqueous solution.

The factors affecting the conformation of the pentafuranose rings of nucleosides in solution have extensively been investigated during the last years by Chattopadhyaya and co-workers [12,13]. The sugar moieties of nucleosides are involved in a two-state N \leftrightarrow S pseudorotational equilibrium that in the case of purine

2'-deoxy- β -D-ribonucleosides is mainly influenced by the *gauche* effect of the O(4')-C(4')-C(3')-O(3') fragment. This *gauche* effect is the strongest factor responsible for driving the N \leftrightarrow S pseudorotational equilibrium to the S-type conformations [12,13]. In the case of purine β -D-ribonucleosides the situation is more complicated because the N \leftrightarrow S equilibrium is additionally controlled by the *gauche* effects of the O(4')-C(1')-C(2')-O(2') and N(9)-C(1')-C(2')-O(2') fragments. The relative populations of various conformers are also influenced by the anomeric effect and by electronic peculiarities of the base [14-16].

The conformation of c^1A_d (1) in D₂O and DMSO solutions was studied by ¹H and ¹³C NMR spectroscopy (see Experimental, Tables 5 and 6). An analysis of the conformational behaviour of the furanose ring of c^1A_d in both solvents was performed by the PSEUROT (version 6.2) program [17-19] which calculates best fits of experimental ³J(H,H) values (³J_{1',2'}, ³J_{1',2''}, ³J_{2',3'}, ³J_{2'',3'} and ³J_{3',4'}) to the five conformational parameters (P and ϕ_m for both N- and S-type conformers and corresponding mole fractions) (Table 4). The electronegativity values for the substituents on H-C-C-H fragments of the furanose rings were taken from the user's manual of the program for D₂O and DMSO solutions. The conformational analysis was evaluated by the PSEUROT analysis of ³J(H,H) values, thereby the ϕ_m values for N and S type rotamers have first been fixed to identical values from 29° to 40° in 1° steps. Further optimization was performed by changing the P value of the minor conformer by 1° constraining then its P and ϕ_m , while P and ϕ_m of the major conformer were calculated. Final optimization was performed in a similar way, by changing the ϕ_m value of the minor conformer by 1° constraining its P and ϕ_m . The PSEUROT optimizations gave low rms error and small individual deviations between experimental and calculated ³J(H,H) coupling constants. The resulting optimized geometries of N and S pseudorotamers for c^1A_d are presented in Table 4. Data for c^1A are included in Table 4 for comparison.

The populations of the staggered rotamers across the C(4')-C(5') bond (torsion angle γ) were calculated from ³J(H(4'),H(5')) and ³J(H(4'),H(5'')) according to Haasnoot *et al.* [20]. The data are presented in Table 4. The pseudorotational parameters P and ϕ_m as well as relative populations of the S- and N-type pseudorotamers of c^1A_d are very similar for both solutions. An analogous conformational behaviour of a furanose ring independent from the solvent's nature was previously documented [21-24]. Moreover, the distribution of the N- and S-type rotamers is practically the same as it was previously found for 1-deazaadenosine and its 2'- and 3'-O-methyl derivatives [10,11].

Table 4. Pseudorotational parameters of 1-deaza-2'-deoxyadenosine (1) and 1-deazaadenosine (2).

Comp.	$\phi_{m,N}$	P _N	$\phi_{m,S}$	P _S	rms	$ \Delta J_{max} $	%S	+sc	ap	-sc
1 ^a	40.0	-10.0	31.9	159.2	0.022	0.03	78	80	20	< 1
1 ^b	44.0	-4.0	30.7	165.4	0.096	0.13	81	41.5	22.5	36
2 ^a	38.0	11.0	30.0	163.9	0.000	0.02	82	79	21	< 1

^a D₂O. ^b d₆-DMSO. The values of P_N and $\phi_{m,N}$ for the minor N-conformer were fixed during the final calculations.

As it can be expected, the $N \leftrightarrow S$ equilibrium is strongly shifted towards the S-type rotamers in accordance with the *gauche* effect of the O(4')-C(4')-C(3')-O(3') fragment. The high relative population of the $+sc$ conformation (*ca.* 80%) across the C(4')-C(5') bond in D₂O solution point to the formation of the intramolecular (5')CH₂OH...N(3) hydrogen bond [10,11,25]. The preference of this conformation is markedly diminished in d₆-DMSO solution. Despite this, the 5'-hydroxyl group of c¹A_d shows a doublet of doublets in its ¹H NMR spectrum in d₆-DMSO solution implying a constrained conformation about the C(4')-C(5') bond which may be accounted for the formation of the intramolecular (5')CH₂OH...N(3) hydrogen bond. Remarkably, the formation of such a hydrogen bond was not proved, to our knowledge, in aqueous or DMSO solutions of adenosine and 2'-deoxyadenosine [26]. As suggested previously from our NMR study on the 6-substituted 1-deazapurine nucleosides, the formation of this intramolecular hydrogen bond is strongly influenced by the increased π -electron density of the pyridine system of 1-deazapurine vs. the pyrimidine system of purines [11].

The conformation of the base about the glycosyl bond was also investigated by means of ¹³C NMR spectroscopy. The vicinal ³J(C(4),H(1')) and ³J(C(8),H(1')) couplings unambiguously prove the predominant *syn*-conformation about the glycosyl bond (Table 6) [27,28] which is in agreement with the NOE data [10,11]. Again, these conformational peculiarities of c¹A_d correspond well with the spatial arrangements of 1-deazaadenosine and its 2'- and 3'-O-methyl derivatives in the solution [10,11]. It should be mentioned that the results of quantum-mechanical calculations predict a stability zone in the *syn*-region of the C-3'-*exo* purine β -D-ribo-nucleosides in which an intramolecular hydrogen bond between the sugar and the base can be formed [29].

Table 5. ¹³C NMR Chemical shifts (δ_{TMS} , ppm) of the 1-deaza-2'-deoxyadenosine (1) and 1-deazaadenosine (2) ^a.

Comp.	C(6) ^b	C(5)	C(3a)	C(7a)	C(7)	C(2)
	C(1) ^c	C(2)	C(4)	C(5)	C(6)	C(8)
1	102.3	144.2	146.4	123.6	147.2	139.4
2 [11]	102.4	144.2	146.5	123.8	147.4	140.0
	C(1')	C(2')	C(3')	C(4')	C(5')	
1	84.5	DMSO	71.4	88.1	62.1	
2 [11]	88.7	72.9	71.1	86.2	62.1	

^a Temp., 303 K; solvent, d₆-DMSO; 125 MHz. ^b Systematic numbering. ^c Purine numbering.

Apart from the very special conformational properties of the monomeric 1-deazaadenine nucleosides the base shows an unusual behavior when incorporated in oligonucleotides. Due to the absence of nitrogen-1 the 1-deazaadenine moiety decreases the stability of a Watson-Crick base pair and increases Hoogsteen base pair stability. This was substantiated by the finding that the replacement of only one dA-residue by c¹A_d (A*) within the duplex 5'-d(TAGGTA*AATACT) · 3'-d(ATCCATTTATGA) decreased the T_m-value from 41°C to 26°C. Contrary to this, the incorporation of three 1-deazaadenine bases into the oligonucleotide 5'-[dG-A-G-A*-G-A-

G-A*-G-A-G-A*-G-A-G)]₂ resulted in a duplex stabilization of 5°C. A parallel duplex is formed by Hoogsteen-Hoogsteen base pairs (Fig. 4) in a similar way as reported for the corresponding oligonucleotide containing adenine [30,31].

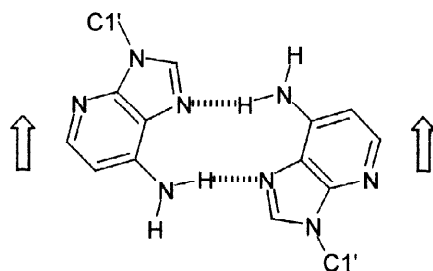


Figure 4. Hoogsteen-Hoogsteen base pair of two c^1A_d residues.

Table 6. C,H-Coupling constants (J , Hz) of 1-deaza-2'-deoxyadenosine (1) and 1-deazaadenosine (2)^a.

C,H-Coupling constant	c^1A_d (1)	c^1A (2)
$^1J(C(1),H(1))$	160.4	160.7
$^2J(C(1),H(2))$	8.9	14.1
$^3J(C(1),NH_2)$	5.5	4.2
$^1J(C(2),H(2))$	174.9	174.6
$^2J(C(2),H(1))$	2.4	2.1
$^3J(C(4),H(2))$	14.1	14.7
$^3J(C(4),H(8))$	4.0	4.6
$^3J(C(4),H(1'))$	4.0	4.6
$^3J(C(5),H(1))$	11.2	11.3
$^3J(C(5),NH_2)$	5.6	5.4
$^3J(C(5),H(8))$	5.6	5.4
$^2J(C(6),H(1))$	8.6	8.3
$^1J(C(8),H(8))$	210.4	211.0
$^3J(C(8),H(1'))$	3.7	2.8
$^1J(C(1'),H(1'))$	163.8	162.9
$^1J(C(2'),H(2'))$	–	147.1
$^1J(C(3'),H(3'))$	150.8	148.8
$^1J(C(4'),H(4'))$	147.4	150.0
$^1J(C(5'),H(5'))$	140.2	128.0

^a Temp., 303 K; solvent, d_6 -DMSO; 125 MHz.

EXPERIMENTAL

^1H NMR Spectra: AC 250 and AMX 500 Spectrometer (Bruker, Germany). ^{13}C NMR Spectra: AMX 500 Spectrometer (Bruker, Germany). δ -Values in ppm and J -values in Hz. The $^3J(\text{H,H})$ coupling constants of the D_2O spectra were simulated and iterated by the WinDaisy program package (Bruker, Germany).

The c^1A_d (**1**) was prepared according to [8]. ^1H NMR (d_6 -DMSO; 500 MHz): 2.23 (ddd, $J_{\text{H-2}'}$ 13.07, $J_{\text{H-1}'}$ 5.99, $J_{\text{H-3}'}$ 2.41, H-2''), 2.79 (ddd, $J_{\text{H-2}''}$ 13.31, $J_{\text{H-1}'}$ 8.02, $J_{\text{H-3}'}$ 5.50, H-2'), 3.56 (ddd, $J_{\text{H-5}'}$ 11.78, $J_{\text{H-4}'}$ 3.91, $J_{\text{OH-5}'}$ 7.73, H-5''), 3.66 (ddd, $J_{\text{H-5}''}$ 11.92, $J_{\text{H-4}'}$ 3.97, $J_{\text{OH-5}'}$ 3.97, H-5'), 3.93 (ddd, $J_{\text{H-5}'}$ 3.61, $J_{\text{H-5}''}$ 3.61, $J_{\text{H-3}'}$ 2.27, H-4'), 4.44 (m, H-3'), 5.21 (d, $J_{\text{H-3}'}$ 3.91, OH-3'), 5.61 (dd, $J_{\text{H-5}'}$ 7.47, $J_{\text{H-5}''}$ 4.21, OH-5'), 6.43 (s, NH_2), 6.40 (dd, $J_{\text{H-2}'}$ 7.68, $J_{\text{H-2}''}$ 6.32, H-1'), 6.41 (d, $J_{\text{H-6}}$ 5.58, H-5), 7.81 (d, $J_{\text{H-5}}$ 5.54, H-6), 8.25 (s, H-2).

^1H NMR (D_2O ; 250 MHz): δ = 2.26 (ddd, $J_{\text{H-2}'}$ 14.05, $J_{\text{H-1}'}$ 6.17, $J_{\text{H-3}'}$ 2.84, H-2''), 2.58 (ddd, $J_{\text{H-2}''}$ 14.05, $J_{\text{H-1}'}$ 8.00, $J_{\text{H-3}'}$ 5.94, H-2'), 3.54 (dd, $J_{\text{H-5}'}$ 12.69, $J_{\text{H-4}'}$ 4.04, H-5''), 3.59 (dd, $J_{\text{H-5}'}$ 12.69, $J_{\text{H-4}'}$ 2.98, H-5'), 3.95 (ddd, $J_{\text{H-5}''}$ 2.98, $J_{\text{H-5}''}$ 4.04, $J_{\text{H-3}'}$ 2.54, H-4'), 4.40 (ddd, $J_{\text{H-4}'}$ 2.54, $J_{\text{H-2}'}$ 5.94, $J_{\text{H-2}''}$ 2.84, H-3'), 6.21 (dd, $J_{\text{H-2}'}$ 8.00, $J_{\text{H-2}''}$ 6.17, H-1').

The c^1A (**2**) was prepared according to Mizuno *et al.* [32]: ^1H NMR (d_6 -DMSO; 250 MHz): δ = 8.23 (s, 1 H, H-2), 7.77 (d, J 4.61, 1 H, H-5), 6.48 (s, 2 H, NH_2), 6.38 (d, J 4.12, 1 H, H-6), 6.08 (m, 1 H, OH-5'), 5.86 (d, J 5.91, 1 H, H-1'), 5.36 (m, 1 H, OH-2'), 5.14 (m, 1 H, OH-3'), 4.70 (m, 1 H, H-2'), 4.12 (m, 1 H, H-3'), 3.97 (m, 1 H, H-4'), 3.57 (m, 2 H, H₂-5').

^1H NMR (D_2O ; 250 MHz): δ = 3.76 (dd, $J_{\text{H-5}'}$ 12.84, $J_{\text{H-4}'}$ 3.25, H-5''), 3.83 (dd, $J_{\text{H-5}''}$ 12.84, $J_{\text{H-4}'}$ 2.49, H-5'), 4.23 (ddd, $J_{\text{H-5}''}$ 3.25, $J_{\text{H-5}'}$ 2.49, $J_{\text{H-3}'}$ 2.38, H-4'), 4.34 (dd, $J_{\text{H-4}'}$ 2.38, $J_{\text{H-2}'}$ 5.21, H-3'), 4.78 (dd, $J_{\text{H-3}'}$ 5.21, $J_{\text{H-1}'}$ 6.78, H-2'), 6.00 (d, $J_{\text{H-2}'}$ 6.78, H-1').

X-Ray crystal structure

Single crystals (size: $0.34 \times 0.32 \times 0.14$ mm c^1A_d (**A**, plates), $0.30 \times 0.10 \times 0.10$ mm c^1A_d (**B**, needles) and $0.76 \times 0.33 \times 0.31$ mm c^1A (**2**)), were prepared as described and fixed at the top of a Lindemann capillary with epoxy resin.

Crystal data

The c^1A_d ($\text{C}_{11}\text{H}_{14}\text{N}_4\text{O}_3$, plates, **A**): orthorhombic; space group $\text{P}2_12_12_1$ (No. 19), $a = 6.720(2)$, $b = 10.299(3)$, $c = 17.024(9)$ Å, $V = 1178.2(8)$ Å³, $Z = 4$, $D_x = 1.411$ Mg m⁻³, Mo-K α radiation ($\lambda = 0.71073$ Å), $\mu = 0.106$ mm⁻¹, $F(000) = 528$, $T = 293(2)$ K.

c^1A_d ($\text{C}_{11}\text{H}_{14}\text{N}_4\text{O}_3$, needles, **B**): orthorhombic; space group $\text{P}2_12_12_1$ (No. 19), $a = 4.888(1)$, $b = 10.685(1)$, $c = 22.034(2)$ Å, $V = 1150.8(3)$ Å³, $Z = 4$, $D_x = 1.444$ Mg m⁻³, Mo-K α radiation ($\lambda = 0.71073$ Å), $\mu = 0.108$ mm⁻¹, $F(000) = 528$, $T = 293(2)$ K.

The c^1A ($C_{11}H_{14}N_4O_4 \cdot H_2O$, **2**): orthorhombic; space group $P2_12_12_1$ (No. 19), $a = 6.866(1)$, $b = 7.956(1)$, $c = 22.779(1)$ Å, $V = 1244.5(3)$ Å³, $Z = 4$, $D_x = 1.517$ Mg m⁻³, Mo-K α radiation ($\lambda = 0.71073$ Å), $\mu = 0.121$ mm⁻¹, $F(000) = 600$, $T = 293(2)$ K.

Data collection and processing

Data for all three compounds were collected on a Siemens P4 four-circle diffractometer with Mo-K α radiation and graphite monochromator.

c^1A_d , plates (**A**): a total of 2523 reflections were collected in a range of $2.31^\circ \leq \theta \leq 24.05^\circ$, giving 1816 independent reflections [$R(\text{int}) = 0.0381$]. The data were not corrected for absorption effects.

c^1A_d , needles (**B**): a total of 2356 reflections were collected in a range of $4.27^\circ \leq \theta \leq 26.99^\circ$, giving 2203 independent reflections [$R(\text{int}) = 0.0319$]. An absorption correction was carried out using psi-scans ($T_{\text{min}} = 0.2417$, $T_{\text{max}} = 0.2699$).

c^1A (**2**): a total of 2523 reflections were collected in a range of $1.79^\circ \leq \theta \leq 24.98^\circ$, giving 2132 independent reflections [$R(\text{int}) = 0.0279$]. An absorption correction was carried out using psi-scans ($T_{\text{min}} = 0.8533$, $T_{\text{max}} = 0.9281$).

Solution and refinement

All structures were solved by standard direct methods. Full-matrix least-squares refinements based on F_o^2 were performed with non-hydrogen atoms assigned anisotropic thermal parameters.

All hydrogen atoms were found in Difference Fourier syntheses, but were constructed in geometrically reasonable positions (bond lengths, bond angles). Especially, the planar geometry of the amino groups and their orientation relative to the ring atoms was confirmed from Difference Fourier synthesis. For all hydrogen atoms a common isotropic thermal parameter was refined.

Programs from the Siemens SHELXTL program package [33,34] were used for the solution, refinement and graphical representation of the structures.

c^1A_d , plates (**A**): a total of 171 parameters was refined, so that a data / parameter ratio of 10.6 results. The final R_1 - and wR_2 - values for data with $I > 2\sigma(I)$ were 0.0479 and 0.1377. Corresponding values for all data were 0.0519 and 0.1423. The goodness-of-fit based on F_o^2 was 1.087. The absolute structure could not be determined reliably from the X-ray data due to the lack of heavy atoms. The final difference Fourier map had a peak maxima and a minima at 0.151 and -0.201 e Å⁻³, without any stereochemical relevance.

c^1A_d , needles (**B**): a total of 171 parameters were refined, so that a data / parameter ratio of 12.9 results. The final R_1 - and wR_2 - values for data with $I > 2\sigma(I)$ were 0.0487 and 0.1070. Corresponding values for all data were 0.0692 and 0.1191. The goodness-of-fit based on F_o^2 was 1.028. The absolute structure could not be determined reliably from the X-ray data due to the lack of heavy atoms. The final difference Fourier map had peak maxima and minima at 0.142 and -0.147 e Å⁻³, without any stereochemical relevance.

1A (2): a total of 190 parameters was refined, so that a data / parameter ratio of 11.2 results. The final R_1 - and wR_2 - values for data with $I > 2\sigma(I)$ were 0.0387 and 0.0904. Corresponding values for all data were 0.0479 and 0.0959. The goodness-of-fit based on F_o^2 was 1.074. The absolute structure could not be determined reliably from the X-ray data due to the lack of heavy atoms. The final difference Fourier map had a peak maxima and a minima at 0.158 and -0.167 e \AA^{-3} , without any stereochemical relevance.

Further details of the structural investigations (excluding structure factors) have been deposited at the Cambridge Crystallographic Data Centre (CCDC) (35).

ACKNOWLEDGEMENTS

We thank Dr. H. Rosemeyer for the measurements of the NMR spectra and for helpful discussions. I.A.M. is deeply grateful for support of the Alexander von Humboldt-Stiftung (Bonn – Bad Godesberg, Germany). Financial support (F.S.) by the Deutsche Forschungsgesellschaft is gratefully acknowledged.

REFERENCES

1. Cristalli, G.; Eleuteri, A.; Vittori, S.; Volpini, R.; Camaioni, E.; Lupidi, G. *Drug Develop. Res.* **1993**, *28*, 253.
2. Vittori, S.; Volpini, R.; Camaioni, E.; Palu, G.; Cristalli, G. *Nucleosides Nucleotides* **1995**, *14*, 603.
3. Cristalli, G.; Franchetti, P.; Grifantini, M.; Vittori, S.; Klotz, K.-N.; Lohse, M.J. *J. Med. Chem.* **1988**, *31*, 1179.
4. Siddiqui, S.M.; Jacobson, K.A.; Esker, J.L.; Olah, M.E.; Ji, X.; Melman, N.; Tiwari, K.N.; Secrist III, J.A.; Schneller, S.W.; Cristalli, G.; Stiles, G.L.; Johnson, C.R.; IJzerman, A.P. *J. Med. Chem.* **1995**, *38*, 1174.
5. Ikehara, M.; Fukui, T.; Uesugi, S. *J. Biochem.* **1974**, *76*, 107.
6. Seela, F.; Wenzel, T.; Debelak, H. *Nucleosides Nucleotides* **1995**, *14*, 957.
7. Seela, F.; Debelak, H.; Rosemeyer, H.; Thomas, H.; Wenzel, T.; Zulauf, M. *Nucleic. Acids Res. Symp. Ser. No. 31*, **1994**, 151.
8. Seela, F.; Wenzel, T. *Helv. Chim. Acta* **1994**, *77*, 1485.
9. Seela, F.; Debelak, H.; Usman, N.; Burgin, A.; Beigelman, L. *Nucleic Acids Res.* **1998**, *26*, 1010.
10. Seela, F.; Debelak, H.; Reuter, H.; Kastner, G.; Mikhailopulo, I.A. *Nucleosides Nucleotides* **1998**, *17*, 729.
11. Mikhailopulo, I.A.; Kalinichenko, E.N.; Podkopaeva, T.L.; Wenzel, T.; Rosemeyer, H.; Seela, F. *Nucleosides Nucleotides* **1996**, *15*, 445.

12. Plavec, J.; Tong, W.; Chattopadhyaya, J. *J. Am. Chem. Soc.* **1993**, *115*, 9734.
13. Thibaudeau, C.; Plavec, J.; Chattopadhyaya, J. *J. Org. Chem.* **1996**, *61*, 266.
14. Uhl, W.; Reiner, J.; Gassen, H.G. *Nucleic Acids Res.* **1983**, *11*, 1167.
15. Rosemeyer, H.; Seela, F. *J. Chem. Soc., Perkin Trans. 2* **1997**, 2341.
16. Seela, F.; Rosemeyer, H.; Zulauf, M.; Chen, Y.; Kastner, G.; Reuter, H. *Liebigs Ann./Recueil* **1977**, 2525.
17. van Wijk, J.; Altona, C. "PSEUROT 6.2 - A program for the conformational analysis of the five-membered rings", University of Leiden, July **1993**.
18. Haasnoot, C.A.G.; de Leeuw, F.A.A.M.; Altona, C. *Tetrahedron* **1980**, *86*, 2783.
19. Rinkel, L.J.; Altona, C. *J. Biomol. Struct. Dyns.* **1987**, *4*, 621.
20. Haasnoot, C.A.G.; de Leeuw, F.A.A.M.; de Leeuw, H.P.M.; Altona, C. *Recl. Trav. Chim. Pays-Bas* **1979**, *98*, 576.
21. Koole, L.H.; Buck, H.M.; Bazin, H.; Chattopadhyaya, J. *Tetrahedron* **1987**, *43*, 2989.
22. Koole, L.H.; Buck, H.M.; Nyilas, A.; Chattopadhyaya, J. *Can. J. Chem.* **1987**, *65*, 2089.
23. Westhof, E.; Röder, O.; Croneiss, I.; Lüdemann, H.-D. *Z. Naturforsch.* **1975**, *30c*, 131.
24. Westhof, E.; Plach, H.; Cuno, I.; Lüdemann, H.-D. *Nucleic Acids Res.* **1977**, *4*, 939.
25. Kitano, S.; Mizuno, Y.; Ueyama, M.; Tori, K.; Kamisaku, M.; Ajisaka, K. *Biochem. Biophys. Res. Comm.* **1975**, *64*, 996.
26. Ts'o, P.O.P, Bases, Nucleosides, and Nucleotides, In: *Basic Principles in Nucleic Acid Chemistry* (ed. by P.O.P. Ts'o), Academic Press, New York and London, 1974, vol. 1, pp. 454-584.
27. Akhrem, A.A.; Mikhailopulo, I.A.; Abramov, A.F. *Org. Magn. Reson.* **1979**, *12*, 247.
28. Davies, D.B. *Prog. Nucl. Magn. Reson. Spectrosc.* **1978**, *12*, 135.
29. Berthod, H.; Pullman, B. *Biochim. Biophys. Acta* **1971**, *232*, 595.
30. Robinson, H.; van Boom, J.H.; Wang, A.H.-J. *J. Am. Chem. Soc.* **1994**, *116*, 1565.
31. Rippe, K.; Fritsch, V.; Westhof, E.; Jovin, T.M. *The EMBO Journal* **1992**, *11*, 3777.
32. Itoh, T.; Sugawara, T.; Mizuno, Y. *Nucleosides Nucleotides* **1982**, *1*, 179.
33. Sheldrick, G.M., SHELXTL, Integrated system for the determination of crystal structures from diffraction data, Rel. 5.03, Siemens 1995.
34. XSCANS, Programm zur Steuerung des Siemens P4-Vierkreisdiffraktometers, Vers. 2.1, Siemens 1994.
35. The atomic co-ordinates for this work are available on request from the Director of the Cambridge Crystallographic Data Centre (CCDC), University Chemical Laboratory, Lensfield Road, Cambridge CB2 IEW, UK. Any request should be accompanied by the full literature citation for this communication. (fax: ++44(1223)336-033, e-mail: deposit@ccdc.cam.ac.uk).